EFDA–JET–PR(13)33

D. Testa, P. Blanchard, T. Panis
and JET EFDA contributors

# On the Measurement of the Radial Profile of the Plasma Isotopic Composition Using Alfvén Eigenmodes

# On the Measurement of the Radial Profile of the Plasma Isotopic Composition Using Alfvén Eigenmodes

D. Testa[1], P. Blanchard[1,2], T. Panis[1]
and JET EFDA contributors*

***JET-EFDA, Culham Science Centre, OX14 3DB, Abingdon, UK***

*[1]Ecole Polytechnique Fédérale de Lausanne (EPFL), Centre de Recherches en Physique des Plasmas (CRPP), Association EURATOM – Confédération Suisse, Lausanne, CH*
*[2]EFDA-CSU, Culham Science Centre, OX14 3DB, Abingdon, OXON, UK*
** See annex of F. Romanelli et al, "Overview of JET Results", (24th IAEA Fusion Energy Conference, San Diego, USA (2012)).*

Preprint of Paper to be submitted for publication in
Nuclear Fusion Letter

**ABSTRACT.**

The measurement of the plasma isotopic composition is necessary in future burning plasma devices such as ITER and DEMO as a tool for optimizing the DT fusion performance. This letter reports on the results of recent experiments performed on the JET tokamak where the radial profile of the plasma isotopic composition was measured using Toroidal Alfvén Eigenmodes (TAEs) with toroidal mode number (N) in the range up to |N| = 15. These results indicate that an active TAE diagnostic system with the capability of operating at multiple frequencies in ITER could provide measurements of the plasma isotopic composition not only supplemental to the standard neutral particle analyser and charge-exchange spectroscopy techniques, but also with the additional and much beneficial features of providing a radial profile of this quantity in real-time, i.e. on a sub-millisecond time base, with a much lower impact on the diagnostic volume occupied ex-vessel.

## 1. INTRODUCTION AND BACKGROUND

The stability properties of Alfvén Eigenmodes (AEs) and the effect of these modes on the energy and spatial distribution of fusion generated alpha particles are among the most important physics issues currently being studied for the operation of burning plasma experiments such as ITER. Additionally, AEs are collective modes that yield information on many background plasma properties, a technique known as *MHD spectroscopy* [1], and this provides a second focus for AE studies.

In the ideal MHD theoretical framework for toroidal plasmas, the continuum frequency spectrum of Alfvén Waves with toroidal mode number N is broken by the coupling of the two poloidal harmonics {M, M+l} due to toroidal effects, where l = {1, 2, …} is an integer number. This leads to the appearance of gaps in the continuum spectrum of AEs, which allows the existence of weakly damped plasma Eigenmodes. The frequency of these gap Eigenmodes is then just given by:

$$F_{AE} = \frac{1}{2\pi} k_{\|}(r) \mathsf{u}_A(r) = \frac{\mathsf{u}_A(r)}{\pi 2 R} \left( N + \frac{M}{q\ r(\ )} \right) = \frac{K(N,q)}{\sqrt{m_p A_{EFF}}} \sqrt{\sum_i n_i} \qquad (1)$$

Here $k_{\|}$ is the parallel wave-vector, $v_A$ is the Alfvén speed, R the torus major radius, q(r) the safety factor profile, r being the minor radius coordinate; $m_p$ is the proton mass and $n_i$ is the density of all the ion species "i" present in the plasmas, including impurities. The function K(N,q) summarizes the dependence of the AE frequency on the toroidal mode number, magnetic configuration, current profile and plasma shape. With $A_i$ the atomic mass of all ion species, eq.(1) shows a clear $1/\sqrt{A_{EFF}}$ dependence of the AE frequency on the plasma effective atomic number, or isotopic composition $A_{EFF}$:

$$A_{EFF} = \sum_i n_i \left( m_i \Big/ m_p \right) \Big/ \sum_i n_i = \sum_i n_i A_i \Big/ \sum_i n_i \qquad (2)$$

Toroidal AEs (TAEs) are the special case of AEs where the coupling occurs between the poloidal

harmonics M and M+1. The peak in the Eigenfunction of ideal TAEs with toroidal mode number N and just the two poloidal components {M, M+1} can be localised at different resonant radial position $r_{RES}$, where we have that $q(r = r_{RES}) = (2M+1)/2N$. Hence the measurement of the AE frequency and toroidal mode number can provide an indication of $r_{RES}$, and in principle allows determining the value of $<A_{EFF}(r_{RES})>$, i.e. the plasma isotopic composition weighted over the mode Eigenfunction centred around $r_{RES}$. Such a measurement is greatly facilitated in plasmas with similar magnetic configurations, current profile and shape, as in this case the function K(N,q) only depends on N and can be easily obtained on a reference set of discharges. Earlier measurements of $A_{EFF}$ in JET using AE spectroscopy of low $|N| = 1$ modes have been proven to agree very well with the data obtained using the low-energy Neutral Particle Analyser (NPA) and the Charge-Exchange (CX) diagnostic systems [1-3].

Accurate measurements of the isotopic composition, and particularly the deuterium/tritium (DT) ratio, are important in future burning plasma experiments such as ITER and DEMO because the power of a fusion reactor is proportional to the product of the densities of deuterons and tritons. Fuel retention in the plasma walls and radial transport of different isotopes are between the main problems that need to be addressed to obtain reliable high-performance operation in tokamaks, particularly when an optimal mixture of deuterium and tritium is intended to be used to produce plasma regimes that aim to achieve a high fusion energy gain [4, 5]. Currently, a combination of a low-energy NPA working as an isotope separator and a high-energy NPA [6] is foreseen as the main diagnostic tool for the measurement of the hydrogen isotope composition in ITER [7]. The main advantage of this technique is that it measures the flux of neutrals exiting the plasmas, which are directly related to the densities of the corresponding ions in the plasma. However, these are rather bulky diagnostic systems that need to be located in the immediate proximity of the vacuum vessel to capture a large enough flux of neutral particles. In the case of the two NPAs currently operating on JET, these systems occupy a volume of a few cubic metres with a weight of a few tonnes. Moreover, NPAs produce a line-integrated measurement that then has to be de-convoluted to obtain a point measurement through a weak energy dependence of the measured neutral fluxes. Their weight and volume then makes it almost impossible to install a number of them to obtain the measurement over multiple lines of sights. The NPA system of the hydrogen isotope composition can be supplemented in ITER with measurements of the Hα/Dα/Tα line intensity ratio, obtained through CX spectroscopy. This technique provides a point-measurement, but the Hα/Dα/Tα lines are related to the presence of atoms, and this is significant only close to the plasma boundary.

AEs are investigated experimentally in JET using an active system, the so-called Alfvén Eigenmodes Active Diagnostic (AEAD), based on a set of two groups of four compact in-vessel antennas located at opposite toroidal positions. The antennas can be powered with a ± relative phasing, producing a frequency-degenerate spectrum, i.e. one with multiple toroidal components for the same antenna driving frequency. The AEAD system provides in real-time, at a 1kHz rate, a direct measurement of the frequency ($f_{MEAS}(N)$), damping rate ($\gamma/\omega(N)$) and amplitude $|\delta B_{MEAS}(N)|$ of the antenna-driven modes during the dynamical evolution of the background plasma parameters,

separately for all toroidal mode numbers up to $|N| \leq 15$ [8-13]. Only one operating frequency range is currently available for the AEAD system, i.e. only one value of $f_{MEAS}(N)$, hence $A_{EFF}$ using eqs.(1,2), can be determined. Note that the AEAD system is currently being upgraded to provide multiple operating frequencies [14].

The radial structure the AE frequency gap provides multiple mode localization at multiple frequencies, even for AEs with the same toroidal mode number. An example of this feature is shown in fig1, using data for the N = 3 TAE obtained with the LEMan code [15, 16] for the JET Pulse No: 77788 at time = 10.096sec. Contrary to the ideal case, in shaped plasmas TAEs have many poloidal components, with poloidal mode numbers usually extending up to the value $M \leq M_{MAX} \approx q_{EDGE}/N$, where $q_{EDGE}$ is the value of the safety factor at the plasma boundary. For this case, only the N = 3 TAE at 171kHz was measured using the AEAD system, as the antenna system excites and detects only one frequency at any one given time, but we see that other N = 3 modes exist in the same toroidal gap at higher frequencies. The dominant poloidal components of this N = 3 mode are M = {3,4,5}, and the maximum in the global Eigenfunction for this mode, i.e. when summed over all poloidal components, is localised in the region $4/3 \leq q_{RES} \leq 3/2$, corresponding to $0.31 \leq s_{RES} \leq 0.49$. The other N = 3 Eigenmodes shown in fig1 at higher frequency are more core-localised towards the plasma centre, as their mode frequency intercepts the continuum before reaching the plasma edge. Hence, in principle we would have been able to measure $\langle A_{EFF}(r_{RES}) \rangle$ for different $r_{RES}$ had the AEAD system been able to use multiple frequencies.

A recent JET experiment [5], where the main ion species was changed-over from deuterium to helium to hydrogen, has provided the opportunity to repeat and extend the earlier measurements of $A_{EFF}$ that were performed using the global N = 1 TAEs to the more reactor-relevant modes with intermediate toroidal mode number up to $|N| = 15$, which are also associated to different resonant positions $r_{RES}$. These new measurements are reported here, with the additional aim to motivate further studies into the use of an active and multi-frequency AE diagnostic system as a supplemental, possibly real-time and radially resolved, diagnostic system for the hydrogen isotope composition in ITER.

This letter is organised as follows. In Section2 we briefly present the experimental scenario and diagnostic techniques used in this work. In Section3 we present the measurements of $A_{EFF}$ for TAEs with different toroidal mode numbers and radial localisation. Finally, in Section4 we present the conclusions from this experimental study and provide some suggestions that may guide future design studies for implementing a diagnostic system for the hydrogen isotope composition in ITER using AEs.

## 2. EXPERIMENTAL SCENARIO AND DIAGNOSTIC TECHNIQUES FOR THE MEASUREMENT OF THE ISOTOPIC COMPOSITION DURING THE JET DEUTERIUM TO HELIUM TO HYDROGEN GAS CHANGEOVER EXPERIMENT.

Following the 1997 JET DTE1 experiment [17], a dedicated, 8-months long clean-up campaign was performed to assess tritium retention and removal strategies [18]: during this campaign the first

measurements of $A_{EFF}$ using the AE spectroscopy method were performed [1, 2]. As during 2010/2011 the JET first wall was changed from carbon to a metallic one (tungsten with beryllium-coated tiles), a main gas changeover experiment from deuterium to helium to hydrogen was performed to provide a reference point for fuel retention studies prior to operation with such a metallic wall. The operational aspects and the main results of this experiment have been previously reported in [5], and the Readers are referred to this publication for further details.

Parasitically to this gas changeover campaign, the AEAD system was used to provide measurements of $A_{EFF}$ using toroidal mode number up to $|N| \leq 15$. The measurements of the mode amplitude, mode frequency and damping rate for this experimental run, and the dependence of the damping rate and mode frequency on $A_{EFF}$, have been already reported elsewhere [19]. The AE data have been analysed for 37 different discharges with a plasma isotopic composition in the range $1.7 \leq A_{EFF} \leq 3.95$, providing in excess of 10'000 individual measurement points, covering a variety of plasma shapes and density, temperature and current profiles. Indicating plasmas with majority species X and minority species Y as X(Y), this experiment was split in four different phases: (a) the reference D2(He4) discharges; (b) the D2(He4) $\rightarrow$ He4(D2) $\rightarrow$ D2(He4) changeover phase; (c) the reference He4(D2) discharges; (d) the He4(D2) $\rightarrow$ H2(He4) changeover phase. The D2(He4) Pulse No: 78978 and the almost pure He4 Pulse No: 79215 are used as reference points for the $A_{EFF}$ measurements reported in this work, leading to the "calibration" of the function K(N,q) appearing in eq.(1) for all measured toroidal mode numbers N up to $|N| \leq 15$. Note that two reference discharges are needed as the background plasma parameters and magnetic configuration are rather different for the first two phases (reference Pulse No: 78978) and the last two phases (reference Pulse No: 79215). The difference is essentially due to the current ramp-up scenario: very fast in Pulse No: 78978, the so called mode-B breakdown, thus allowing entering into an X-point phase early during the discharge, from t = 4.2sec onwards, compared to rather slow in Pulse No: 79215, the so called mode-D breakdown, which then allows entering into an X-point phase late during the discharge, from t = 10.5sec onwards. Hence, without using two different K(N,q) functions, a direct comparison for $A_{EFF}$ calculations between these two operating scenario is not possible as at the same time point the magnetic configuration is different.

Figure2(a,b) show an overview of the main plasma parameters over the active AEAD diagnostic time window for these two reference discharges. In Fig.2, and in the reminder of this work, r is the radial coordinate across the plasma poloidal cross-section and a is the plasma minor radius, the suffixes "0" and "95" indicate a value on the magnetic axis (r/a = 0) and at 95% (r/a = 0.95) of the normalised poloidal flux, and the symbol "<A>" indicates volume averaging of the quantity "A". The EFIT code [20] was used for reconstructing the magnetic equilibrium, complemented with Motional Stark Effect and polarimetry measurements in the plasma core when available: hence the typical uncertainty on the safety factor profile is better than 10% when EFIT has been constrained with core data, or up to 20% otherwise, as determined by comparing the position of the q = 1 surface at the sawtooth crash between the EFIT and the $T_e(r)$ profile data. The electron density and temperature were measured with a high-resolution Thomson Scattering (when available) or a LIDAR diagnostic

system, with typical uncertainties of the order of ±10% in both cases. The ion temperature (not shown in fig.2, as very close to $T_e$) and effective charge were measured using charge-exchange (CX) spectroscopy (when available, with typical uncertainties around 15%) or derived from equilibrium reconstruction using ion-electron energy equi-partition and bremsstrahlung measurements, with typical uncertainties up to 25% in this latter case. Note that all these uncertainties are taken into account for each individual time point when combining the data in our analysis database, as explained later in Section3.

In addition to the background plasma parameters indicated above, the top frame of Fig.2 shows the value of the magnitude of the antenna-driven radial component of the magnetic field ($|\delta B_{ANT}|$) measured with a pick-up coil (T001) mounted on the low-field side vessel wall, the value of the antenna frequency ($f_{ANT}$), and the value ($f_{RT}I_p \propto B_{\phi 0\text{-}RT}/R_{GAP}/q_{GAP}/\sqrt{A_{EFF}}/\sqrt{n_{e0\text{-}RT}}*I_p(t)/\max(I_p)$) of the central frequency of the N = 1 TAE gap computed in real-time using the values $R_{GAP} = 3$m and $q_{GAP} = 1.5$ and a user defined $A_{EFF}$ ($A_{EFF} = 2$ for Pulse No: 78978 and $A_{EFF} = 4$ for Pulse No: 79215). The value of $f_{RT}I_p$ is normalized with respect to the time evolution of the total plasma current to take into account the time evolution of the q-profile. Finally, note that, as for the large majority of the discharges in our database, these reference discharges enter into the X-point phase, at t = 4.2sec for Pulse No: 78978 and at t = 10.5sec for Pulse No: 79215. This is indicated by the large increase at that time point in the edge magnetic shear $s_{95}$ and edge elongation $\kappa_{95}$, which then remain both approximately constant, as shown in the last two frames from the bottom in fig2.

Figure 3(a,b) show the measurement of the AE frequency $f_{MEAS}(N)$ as function of time for the different toroidal mode numbers detected in these discharges, discriminated in real-time and post-pulse using an algorithm based on the Sparse Representation of Signals [21, 22]. In addition to the measured mode frequency, in fig3 we also plot the antenna sweep and the value of the real-time and post-pulse central frequency of the N = 1 TAE gap. Note that disagreement between these two data can easily occur during the current ramp-up phase, due to the fact that the q-profile evolution is correctly taken into account post-pulse, but only approximately in real-time, through the $I_p$ normalization of the TAE frequency.

The $f_{MEAS}(N)$ data are from the post-pulse analysis, which extends up to |N| = 30 as it does not suffer from the CPU and RAM limitations of the real-time processing, limiting the analysis to |N| = 15. The agreement between the real-time and post-pulse $f_{MEAS}(N)$ data is always within <200Hz for all modes up to |N| = 15. The typical uncertainty on the measurement of the mode frequency is within 50Hz, due to the accuracy of the digital synchronous detection system used in the AEAD system. For the accuracy on the determination of the mode numbers we also consider the possible statistical and systematic errors due to the algorithm used to extract such data. For the $A_{EFF}$ measurements reported in Section3 of this work, the toroidal mode number can be determined exactly (i.e. N = N ±0) up to |N| = 10, with an error for higher mode numbers $11 \leq |N| \leq 30$ of at least ±1 and up to ±10%.

In Fig.3 we note, first, that the same N-modes are measured at different frequencies in the two reference discharges, which clearly demonstrate the importance of correctly "calibrating" the factor K(N,q) to extract an accurate value of $A_{EFF}$. Second, we also note that in the same discharge the same

N-mode can be measured at very different frequencies, i.e. at different position in the TAE gap, in line with the LEMan simulations shown in Fig.1. Hence, it is important to correctly determine the value of K(N,q) by using modes at the same position in the frequency gap, using guidance from simulations when available.

## 3. MEASUREMENTS OF THE ISOTOPIC COMPOSITION DURING THE JET DEUTERIUM TO HELIUM TO HYDROGEN GAS CHANGEOVER EXPERIMENT.

The value of the plasma isotopic composition $A_{EFF}$ is obtained from the measurement of the TAE mode frequency $f_{MEAS,N}$ scaled with respect to the relevant reference discharges, the D2(He4) Pulse No: 78978 for the D2 → He4 → D2 changeover, and the almost pure He4 Pulse No: 79215 for the He4 → H2 changeover. Following the procedure detailed in Section-5a in [2], we can start by neglecting the contribution from all plasma impurities. With this approach we have that the nominal value of the plasma isotopic composition $A_{EFF,0}$ is given by the square of the ratio between the measured mode frequency $f_{MEAS,N}$ of a TAE with toroidal mode number N in the reference single main ion (superscript "(1)") and the actual two main ion (superscript "(1,2)") species plasmas:

$$A_{EFF,0} = A_1 \left( \frac{f^{(1)}_{MEAS,N}}{f^{(1,2)}_{MEAS,N}} \right)^2 \tag{3}$$

Further to the analysis presented in [1, 2], here we correct this initial estimate of $A_{EFF}$ to account for the plasma effective charge $Z_{EFF}$. This correction is important as (even trace) impurities with atomic charge $Z_k$ and mass $A_k$ affect considerably the determination of $A_{EFF}$ when $Z_{EFF}$ is sufficiently different from the nominal value that would characterise a pure two main ion species plasmas (with $\{n_1, A_1, Z_1\}$ and $\{n_2, A_2, Z_2\}$). Empirically, this occurs when $Z_{EFF} > 1.3*(n_1 Z_1^2 + n_2 Z_2^2)/|Z_e|/n_e$. Using the approximation of low-Z trace impurities $n_k/n_e = o(1)$ and $(Z_{EFF} - \max(Z_1, Z_2))/\max(Z_1, Z_2) = o(1)$, we have that:

$$A_{EFF} \approx A_{EFF,0} \left[ 1 + \frac{Z_*}{n_e A_1} \left( 1 - \frac{A_1}{A_{EFF,0}} \right) \sum_k n_k A_k \right] = A_{EFF,0} (1 + \Delta A_{EFF}). \tag{4}$$

In eq.(4) the index k indicates all the (trace) impurity species with density $n_k$, and $\Delta A_{EFF}$ is the impurity correction to $A_{EFF}$, proportional to the non-ideal quantity $Z_* = |Z_e|(Z_1 + Z_2 - Z_{EFF})/Z_1/Z_2$. Note that for a pure two main ion species plasmas, i.e. with $n_k = 0$ for all impurities species, we have that $Z_* = (n_1 + n_2)/n_e$.

Figure 4 shows the measurement of the plasma isotopic composition for Pulse No: 79216, another almost pure He4 discharge with background plasma parameters very similar to Pulse No: 79215. For this discharge we show the $A_{EFF}$ data using N = 3 and N = 7 TAEs, in comparison with the data from CX spectroscopy. The reference frequency data used to calibrate the factor K(N,q) in eq.(1) and obtain $A_{EFF}(N)$ are taken from the Pulse No: 79215. For fig4 the AE Eigenfunction was calculated using the fluid version of the CASTOR code [23] as it is much faster than the gyro-kinetic

code LEMan, thus efficiently allowing for all the Eigenfunction calculations that were needed for this work. Note that the Eigenfunctions from CASTOR and LEMan have been found to be in very good agreement when the same input data are used for the calculations [24].

Remembering that the $A_{EFF}(N)$ data represent a measurement averaged over the mode Eigenfunction, with the location of its peak indicated as $r_{RES}$ in Fig.4, we note that there is a good agreement between the CX and the TAE data during the current flat-top phase, from t = 6sec onwards. Conversely, during the current ramp-up phase the difference is significant but progressively reducing, which is consistent with an influx of gas from the plasma boundary towards the central region of the plasma. Finally, we note that there is a small, but systematic difference in $A_{EFF}$ for the N = 3 and the N = 7 mode seen during the current flat-top phase, up to about 2sec after the X-point formation, which occurs at t = 10.5sec. This is consistent with the two Eigenmodes having a slightly different $r_{RES}$, thus indicating an isotopic dependence of the radial density profiles of the different in species. Figure5 shows the measurement of the evolution of the plasma isotopic composition and effective charge during the gas change-over experiment analysed here. The nominal values for $A_{EFF}$ and $Z_{EFF}$ shown in fig5 are obtained from the requested input gas flux of {H2, D2, He4}, and we show two measurements of $A_{EFF}$ from TAE spectroscopy, one for higher $N \geq 7$, more core localized modes, with peak Eigenfunction in the region $0.15 < r_{RES}[m] < 0.42$, and one for lower $N \leq 3$, more global modes, with peak Eigenfunction in the region $0.35 < r_{RES}[m] < 0.62$. Note that the TAE and CX data were also averaged over the time interval of the TAE measurements. As an order-zero observation, the trends in $A_{EFF}$ and $Z_{EFF}$ are very similar: obviously plasmas with higher effective atomic number must also have higher effective charge. First, we find that the nominal $Z_{EFF}$ value is always lower than the CX value, the difference being only partly accounted for by the contribution of high-Z impurities. This is consistent with the rather obvious fact that the input gas flux of {H2, D2, He4} does not provide a good indication of $Z_{EFF}$. This is also true for the $A_{EFF}$ data, as the nominal values are always lower than the CX and TAE measurements. Second, we find that the evolution of the plasma isotopic composition is well measured with both CX and TAE data, and this is particularly evident during the last phase of the experiments, i.e. the He4 → H2 changeover, where $A_{EFF}$ changes from that of an almost-pure He4 plasma, $A_{EFF} > 3.5$, to that of an majority H2 plasma, $A_{EFF} \approx 1.5$. Hence, we are satisfied that the TAE diagnostic can provide sufficiently accurate measurements of $A_{EFF}$ over a variety of plasma conditions, which are not so sensitive to the details of equilibrium and plasma shape once a reference discharge and the role of impurities are correctly taken into account. It is important to note here that during the D2 → He4 → D2 changeover phase the $A_{EFF}$ measurement using TAEs relies on the presence of impurities and isotopic dependence of density profiles of different ion species. This is straightforward to understand using charge neutrality for pure D2 and pure He4 plasmas with the same electron density profile. Since $n_e(r) = Z_D n_D(r) = Z_{He4} n_{He4}(r)$ at every radial position, and $A_{He4}/Z_{He4} = A_D/Z_D$, the TAE frequency for any N-mode is nominally exactly the same in pure D2 and pure He4 plasmas. However, the plasma effective charge $Z_{EFF} = \Sigma_i n_i Z^2_i / |Z_e| / n_e = \{Z_D, Z_{He4}\}$ is not the same in pure D2 and pure He4 plasmas, and this allows distinguishing between them.

Figure 6 shows the measurement of the plasma isotopic composition as function of the nominal value of $A_{EFF}$. First, note that the CX spectroscopy data, giving $A_{EFF}$ at the plasma boundary, are almost always larger than the TAE data, which sample also the more central regions of the plasmas. Second, the $A_{EFF}$ data for the global N≤3 TAEs are also almost always larger than those for the more core-localized global N≥7 TAEs. This suggests that recycling from the wall and the ensuing particle transport towards the plasma core play a rather significant role in determining the radial profile of $A_{EFF}$. This can only be addressed using a diagnostic that provides some sort of localization for the $A_{EFF}$ measurements, such as the TAE system, even if the radial resolution is not particularly fine. Finally, we note that the difference between the CX and TAE measurements is larger for lower nominal values of $A_{EFF}$, being practically negligible for $A_{EFF}$>3. This suggests that recycling and accumulation of high-Z impurities from the walls in the edge region of the plasma might have an isotopic dependence, whereby wall efflux and transport of such high-Z impurities from the plasma boundary towards the plasma core is lower in plasmas with lower $A_{EFF}$ and $Z_{EFF}$.

**SUMMARY, CONCLUSIONS AND DISCUSSION.**

In summary, we have presented experimental measurements of the plasma isotopic composition using TAEs with different radial localisation, as determined by their peak in their Eigenfunction. These measurements are in good agreement with the more routinely available CX data measuring $A_{EFF}$ at the plasma edge, and provide additional information on the radial profile of $A_{EFF}$ due to the radial localisation of TAEs with different toroidal mode numbers. The TAE measurements indicate that the recycling from the wall and the ensuing particle transport towards the plasma core play a rather significant role in determining the radial profile of $A_{EFF}$. Furthermore, it is suggested that the wall efflux and transport of high-Z impurities from the plasma boundary towards the plasma core is lower in plasmas with lower $A_{EFF}$ and $Z_{EFF}$.

The drawback of the TAE measurement is that they require a set of reference discharges to have been previously established, as $A_{EFF}$ is measured from the difference between the current and the reference discharge in the mode frequency of TAEs with the same toroidal mode number and the same localisation in the TAE frequency gap. Contrary to what happens in current devices, this is actually not a show-stop problem for future burning plasma devices, such as ITER and DEMO, which in fact will essentially work on a much reduced set of standard operating scenarios.

The main advantages of a TAE measurement of $A_{EFF}$, in addition to the radial localisation, is that there is potential for real-time capabilities and the overall volume occupation of the diagnostic is very small compared to that of the NPAs currently foreseen for the $A_{EFF}$ measurements in ITER. Considering the case of JET, the TAE diagnostic system allows measuring the TAE mode frequency in real-time on a 1kHz clock cycle, using two 1m × 35cm × 25cm groups of four antennas each in-vessel, and only light-weight ancillary systems ex-vessel.

The $A_{EFF}$ measurements cannot currently be obtained in real-time in JET with the TAE diagnostic system due to CPU and RAM limitations of the controller, which prevent the loading, in the form of tabulated values, and the processing of the information from the reference discharges that are needed

to compute $A_{EFF}$ from the measured mode frequency for the current discharge. It is foreseeable that with some relatively minor hardware and software upgrades these calculations could be performed in real-time for testing this method in view of possible applications to ITER ad DEMO plasma operation.

**ACKNOWLEDGEMENTS.**

This work was supported by EURATOM under the contract of Association with CRPP-EPFL, and was carried out within the framework of the European Fusion Development Agreement. This work was also partly supported by the Swiss National Science Foundation. The views and opinions expressed herein do not necessarily reflect those of the European Commission. The Authors would like to thank the various members of the CRPP, MIT and JET staff that contributed to the design, installation, commissioning and operation of the AEAD system. Specifically, the authors wish to acknowledge the contribution of T.Loarer (Commissariat à l'Energie Atomique) and C.Giroud and K-D.Zastrow (both at the Culham Centre for Fusion Energy) for the preparation of the JET gas changeover experiment, and of A.Goodyear (Culham Centre for Fusion Energy) and H.Carfantan (Université de Toulouse, Institut de Recherche en Astrophysique et Planétologie) for the development and implementation at JET of the SparSpec code.

**REFERENCES.**

[1]. A. Fasoli et al., *Plasma Physics and Controlled Fusion* **44** (2002), B159.
[2]. A. Fasoli et al., *Physics of Plasmas* **7** (2000), 1816.
[3]. D. Bettella, A. Murari, M. Stamp, D. Testa, *Plasma Physics and Controlled Fusion* **45** (2003), 1893.
[4]. M.Z. Tokar and S. Moradi, *Nuclear Fusion* **51** (2011), 063013.
[5]. T. Loarer et al., *Journal of Nuclear Materials* **415** (2011), S805.
[6]. V.I. Afansyev et al., *Review of Scientific Instruments* **74** (2003), 2338.
[7]. V.I. Afansyev et al., *Plasma Physics and Controlled Fusion* **55** (2013), 045008.
[8]. A. Fasoli et al., *Physical Review Letters* **75** (1995), 645.
[9]. D. Testa, A. Fasoli et al., *The new Alfvén Wave Active Excitation System at JET*, Proceedings 23rd SOFT Conference (2004); weblink: http://infoscience.epfl.ch/record/143354/files/.
[10]. D. Testa, N. Mellet, T. Panis et al., *Nuclear Fusion* **50** (2010), 084010.
[11]. T. Panis, D. Testa, A. Fasoli et al., *Nuclear Fusion* **50** (2010), 084019.
[12]. D. Testa, A. Fasoli, A. Goodyear et al., *Fusion Engineering and Design* **86** (2011), 381.
[13]. D. Testa, H. Carfantan, A. Goodyear et al., *EuroPhysics Letters* **92** (2010), 50001.
[14]. P. Woskov et al. GP8.00129, Proceedings 54th Annual Meeting of the APS Division of Plasma Physics, October 29th –November 2nd 2012, Providence (USA).
[15]. P. Popovich, W.A. Cooper, L.Villard, *Computer Physics Communications* **175** (2006), 250.
[16]. N. Mellet, W.A. Cooper, P. Popovich, L. Villard, S. Brunner, *Computer Physics Communications* **182** (2011), 570.

[17]. M. Keilhaker et al., *Nuclear Fusion* **39** (1999), 209.
[18]. N. Bekris et al., *Journal of Nuclear Materials* **337** (2005), 659.
[19]. D.Testa, T.Panis, P.Blanchard, A.Fasoli, *Nuclear Fusion* **52**(9) (2012), 094006.
[20]. L.L.Lao, H.St.John, R.D.Stambaugh, A.G.Kellman, W.Pfeiffer. *Nuclear Fusion* **25** (1985), 1611.
[21]. S.Bourguignon, H.Carfantan, T.Böhm, *Astronomy and Astrophysics* **462** (2007), 379.
[22]. A.Klein, H.Carfantan, D.Testa et al., *Plasma Physics and Controlled Fusion* **50** (2008), 125005.
[23]. W.Kerner et al, *Journal of Computational Physics* **142** (1998), 271.
[24]. ITPA Group on Energetic Particles, *The Influence of Plasma Shaping on the Damping of Toroidal Alfvén Eigenmodes*, in Fusion Energy 2010 (Proc. 23rd Int. Conf. Daejeon, 2010) (Vienna: IAEA); http://www-naweb.iaea.org/napc/physics/FEC/FEC2010/html/index.htm, CD-ROM: THW/P7-08.

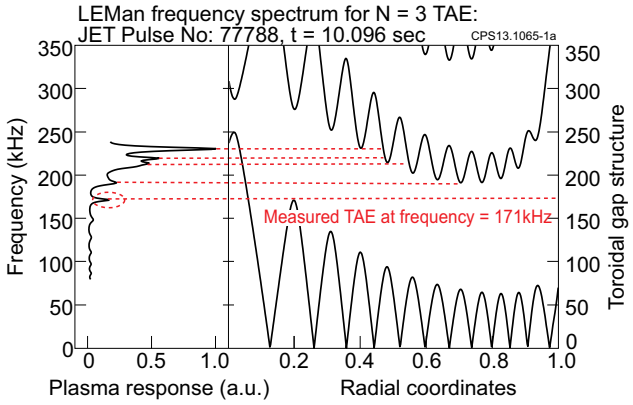


*Figure 1a: Results of the LEMan simulation for the N=3 TAE on Pulse No: 77788 at t = 10.096sec with on axis-parameters: toroidal magnetic field $B_{\phi 0}$ = 2.7T, electron density $n_{e0} = 2.6\times10^{19}m^{-3}$, electron and ion temperatures $T_{e0} = T_{i0} = 2.4$keV. Here we show the frequency scan of the plasma response to the antenna drive (left sub-frame) and the Alfvén branches spectrum computed using the dispersion relation (right sub-frame). For these simulations, all poloidal components from M = –5 to $M_{MAX}$ = 22 have been retained. The radial coordinate s (s = 0 in the centre and s = 1 at the border of the plasma) is defined in the LEMan code as the toroidal flux. The only N = 3 mode directly measured in the experiment is highlighted, and we note that four other N=3 modes appear in the TAE gap at higher frequencies. The measured N = 3 mode at 171kHz intercepts the continuum close to the magnetic axis (s = 0), but extends outwards up to the plasma edge. Conversely, the other N = 3 modes at higher frequency are more core-localised towards the plasma centre, as their mode frequency intercepts the continuum before reaching the plasma edge, in addition to closer to the magnetic axis.*

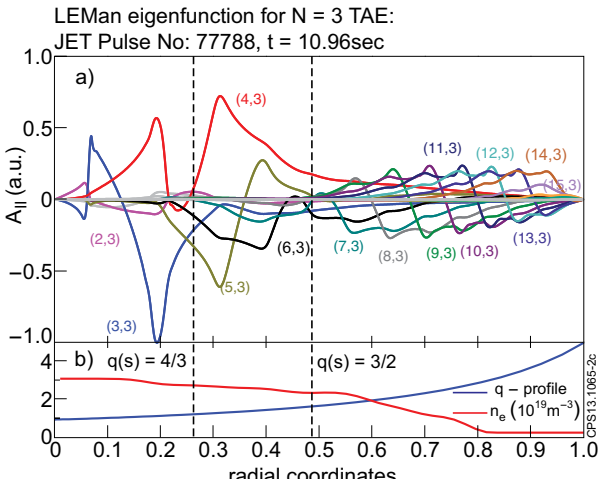


*Figure 1b: Eigenfunction of the parallel component of the vector potential A|| for the measured N = 3 mode at 171kHz shown in fig1a. The dominant poloidal components of this N = 3 mode are M = {3, 4, 5}, and the peak Eigenfunction for this mode is localised in the region 4/3≤qRES≤3/2. In the region closer to the magnetic axis, the Alfvén branches M = 3 to M = 5 intersect with the continuum. This contributes considerably to the power absorption, making the Eigenfunction almost negligible in this region. From s = 0.4 outward the characteristic structure of a global plasma mode is clearly recognizable, with the Eigenfunction extending up to the plasma edge, as it involves a large number of Fourier poloidal components, from M = 5 to at least M = 14.*

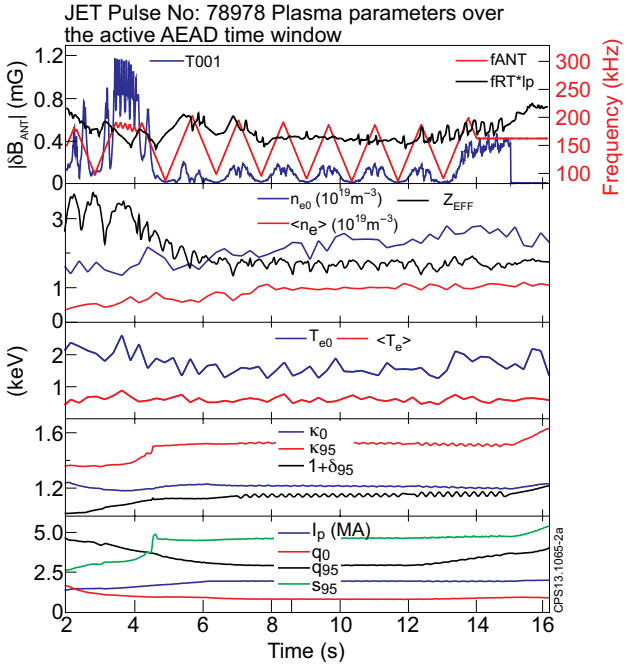


*Figure 2a: Overview of the main plasma parameters over the active AEAD time window for the reference D2(He4) Pulse No: 78978. Here $B_{\phi 0}$ = 2.1T is the toroidal magnetic field on the magnetic axis, $I_p$ = 2MA (flat-top value) is the plasma current, q and s are the safety factor and magnetic shear profiles, κ and δ are the elongation and average top/bottom triangularity profiles, $T_e$ and $n_e$ are the electron temperature and density profiles, and $Z_{EFF}$ is the plasma effective charge. The subscripts "0" and "95" indicate values measured on the magnetic axis and at 95% of the normalised poloidal flux coordinate. The top frame shows the antenna frequency waveforms and the driven magnetic field amplitude at the plasma edge, which are used for the TAE measurements.*

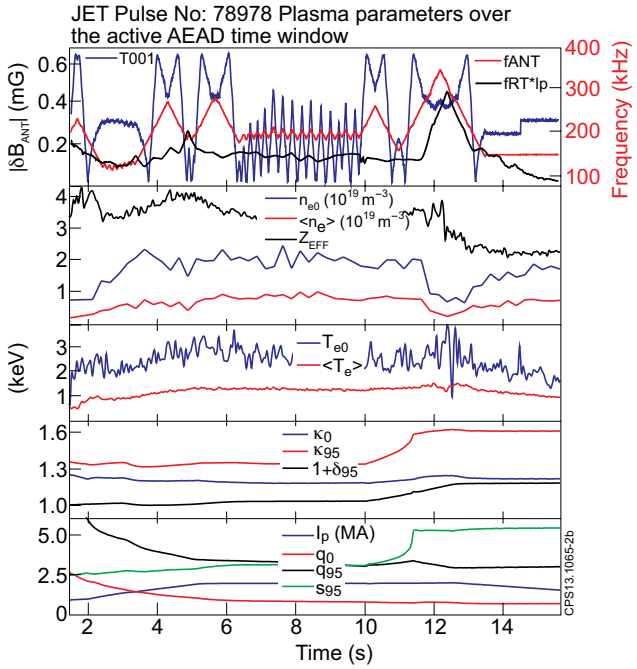


*Figure 2b: Overview of the main plasma parameters over the active AEAD time window for the reference almost pure He4 Pulse No: 79215, using the same notations as in fig.2a. Here is the toroidal magnetic field on the magnetic axis is $B_{\phi 0} = 2.4T$ and the flat-top plasma current is $I_p = 2MA$.*

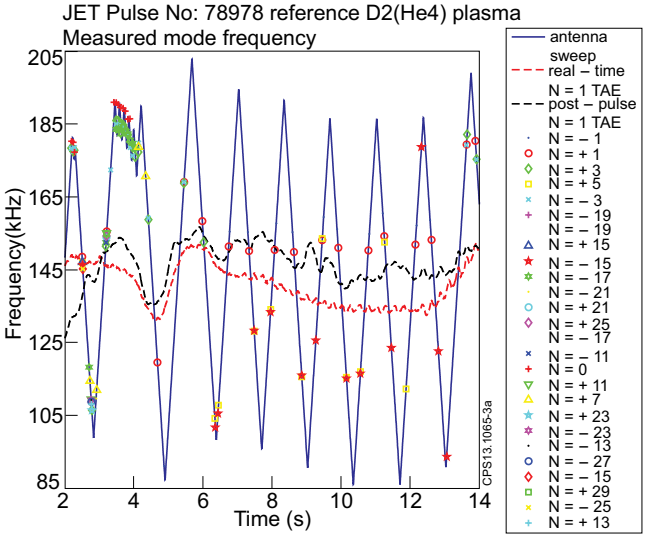


*Figure 3a: Measurement of the mode frequency for TAEs with different toroidal mode numbers for the reference D2(He4) Pulse No: 78978. Here the data from the post-pulse analysis are shown, which extends up to |N| = 30 as it does not suffer from the CPU and RAM limitations of the real-time processing, which limit the real-time analysis to |N|≤15. Different N-modes up to |N| = 30 are obtained using post-pulse analysis at different frequencies over the entire antenna sweep. The agreement between the real-time and post-pulse values of $f_{MEAS}(N)$ data is always within <200Hz for all N-modes up to |N| = 15.*

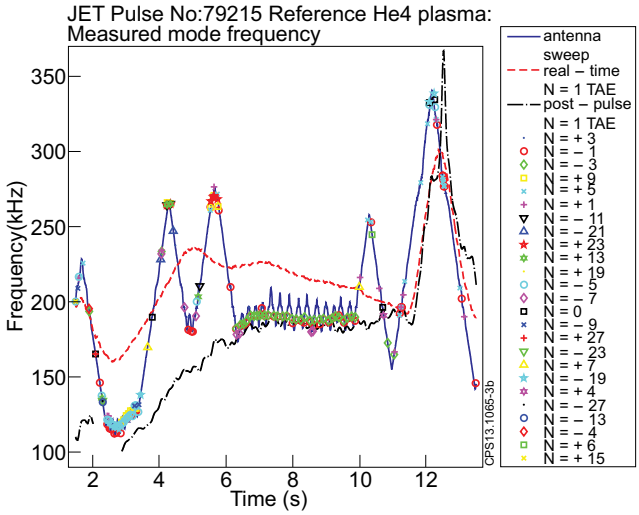


*Figure 3b: Measurement of the mode frequency for TAEs with different toroidal mode numbers for the reference almost pure He4 Pulse No: 79215, using the same notations as in Fig.3a. Different N-modes up to |N| = 30 are obtained at different frequencies over the entire antenna sweep, and the agreement between the real-time and post-pulse $f_{MEAS}(N)$ data is always within <200Hz for all N-modes up to |N|=15. Here the significant difference between the real-time and post-pulse value of the N = 1 frequency during the current ramp-up phase, up to t = 6sec, is due to the fact that the q-profile evolution is correctly taken into account post-pulse, but only approximately in real-time, through the $I_p$ normalization of the TAE frequency.*

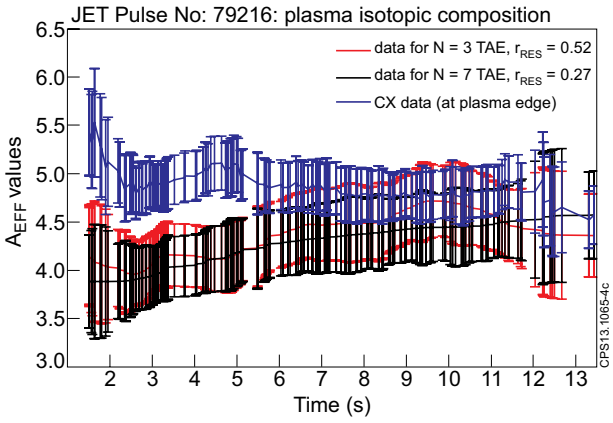


*Figure 4: Measurement of plasma isotopic composition for the Pulse No: 79216 using N = 3 and N = 7 TAEs, in comparison with the data from CX spectroscopy. The reference frequency data used to calibrate the factor K(N,q) in eq.(1) and obtain $A_{EFF}(N)$ are taken from the Pulse No: 79215. The $A_{EFF}(N)$ data represent a measurement averaged over the mode Eigenfunction, summed over all calculated poloidal components, and the location of its peak is indicated as $r_{RES}$ in the figure.*

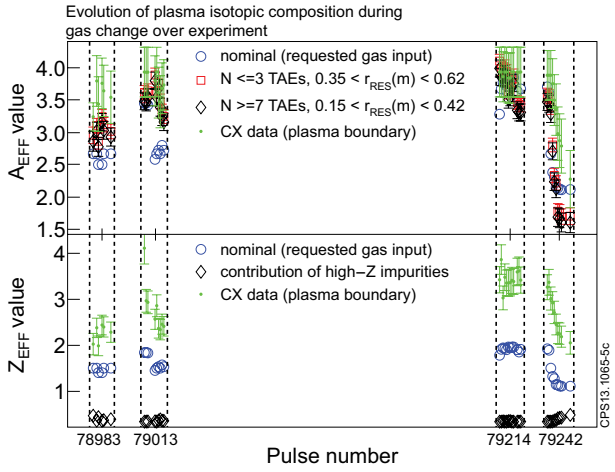


*Figure 5: Measurement of the evolution of the plasma isotopic composition and effective charge during the gas change-over experiment analysed here. Four different phases of the experiment are recognizable, shown by the vertical lines in both sub-plots, and labelled with the central shot number in each phase: (a) the reference D2(He4) Pulse No's: 78978 to 78988; (b) the D2(He4) → He4(D2)→ D2(He4) changeover phase, from Pulse No's: 79007 to 79018; (c) the reference He4(D2) Pulse No's: 79208 to 79220; (d) the He4 → H2 changeover phase, from Pulse No's: 79235 to 79248.*

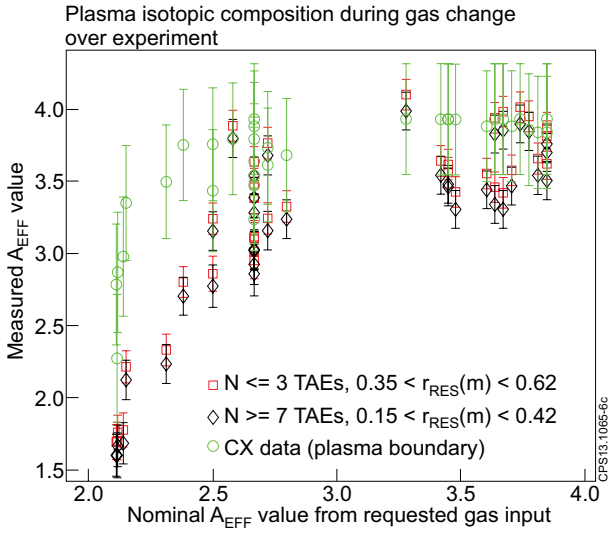


*Figure 6: Measurement of the plasma isotopic composition as function of the nominal value of $A_{EFF}$. The CX spectroscopy data, giving $A_{EFF}$ at the plasma boundary, are almost always larger than the TAE data, which sample also the more central regions of the plasmas. The difference between the CX and TAE measurements is larger for lower nominal values of $A_{EFF}$, being practically negligible for $A_{EFF} > 3$. The $A_{EFF}$ data for the global N≤3 TAEs are also almost always larger than those for the more core-localised global $N \geq 7$ TAEs.*